of temperature variation, etc., must be taken into consideration when one designs the ISG.

Fig. 12 presents dispersion characteristics of both single and coupled versions of the ISG with some typical parameters. The even and odd propagation constants approach the one for the uncoupled guide as the operating frequency gets higher. This phenomenon is due to the decrease of coupling between the two guides at the higher frequencies where the concentration of the fields in the regions above the strips becomes stronger.

Finally, Fig. 13 shows the coupling factor κ for the dominant even and odd modes versus the separation $2s$ of two guides. The parameter κ is defined as

$$\kappa = (k_{ze} - k_{zo})/k_z$$

where k_{ze} and k_{zo} are the propagation constants of the even and odd dominant $E_{11}{}^y$ modes in the coupled structure, while k_z is that of the $E_{11}{}^y$ mode in the uncoupled ($s = \infty$) guide.

V. Conclusion

In this paper, a novel waveguide structure, an ISG, has been analyzed both theoretically and experimentally. This waveguide is believed to be useful for millimeter-wave integrated circuits. Comparisons have been made, where feasible, between theoretical and experimental results and the agreement was found to be good. A number of numerical results useful for designing this type of waveguide are presented in addition to the dispersion diagrams.

Acknowledgment

The author wishes to thank the Fujitsu Laboratories, Kawasaki, Japan, for supplying an IMPATT oscillator and several other millimeter-wave components. He also wishes to thank Dr. T. Rozzi of the University of Illinois, on leave from Phillips Laboratories, The Netherlands, for reading the manuscript.

References

[1] M. V. Schneider, "Millimeter-wave integrated circuits," in *International Microwave Symposium Digest*, pp. 16–18, (Chicago, Illinois, June 4–6, 1973).
[2] R. M. Knox and P. P. Toulios, "A *V*-band receiver using image line integrated circuits," in *Proceedings of the National Electronics Conference*, vol. 29, pp. 489–492, Oct. 16–18, 1974.
[3] P. P. Toulios and R. M. Knox, "Image line integrated circuits for system applications at millimeter wavelengths," U.S. Army Electronics Command, Final Report, Rept. No. ECOM-73-0217-F, July 1974.
[4] H. Jacobs and M. M. Chrepta, "Electronic phase shifter for millimeter-wave semiconductor dielectric integrated circuits," *IEEE Trans. Microwave Theory Tech.*, vol. MTT-22, no. 4, pp. 411–417, April 1974.
[5] T. Itoh and R. Mittra, "New waveguide structures for millimeter-wave integrated circuits," in *International Microwave Symposium Digest*, pp. 277–279, Palo Alto, CA, May 12–14, 1975.
[6] W. McLevige, T. Itoh, and R. Mittra, "New waveguide structures for millimeter wave and optical integrated circuits," *IEEE Trans. Microwave Theory Tech.*, vol. MTT-23, no. 10, Oct. 1975.

Double-Layered Slot Line for Millimeter-Wave Integrated Circuits

NIKOLA SAMARDZIJA AND TATSUO ITOH, SENIOR MEMBER, IEEE

***Abstract*—A new type of waveguide, a double-layered slot line, is described which is useful for millimeter-wave integrated circuits (IC's). Galerkin's method applied in the Fourier transform domain is used for analyzing the propagation characteristics of the dominant mode in the structure. Theoretical and experimental results are presented and compared.**

Manuscript received January 19, 1976; revised May 4, 1976. This work was supported in part by the Joint Services Electronics Program (U.S. Army, U.S. Navy, U.S. Air Force) under Contract DAAB-07-72-C-0259, and in part by the U.S. Army Research Office under Contract DAHCO4-74-G-0113. Part of this paper was presented at the IEEE International Microwave Symposium, Palo Alto, CA, May 12–14, 1975.

N. Samardzija was with the Coordinated Sciences Laboratory and the Department of Electrical Engineering, University of Illinois, Urbana, IL 61801. He is now with the Department of Electrical Engineering, Couren College of Engineering, University of Houston, Houston, TX 77004.

T. Itoh was with the Coordinated Sciences Laboratory and the Department of Electrical Engineering, University of Illinois, Urbana, IL 61801. He is now with the Radio Physics Laboratory, Stanford Research Institute, Menlo Park, CA 94025.

I. Introduction

RECENTLY, considerable interest has been shown for the millimeter-wave integrated circuits (IC's) for use in radiometry, radar, astronomy, and communications. Several types of waveguides convenient for millimeter-wave IC applications have been proposed. They include microstrip line [1], image guide [2], silicon guide [3], and strip dielectric guide [4].

At millimeter-wave frequencies the microstrip line shows a considerable conductor loss, and its dimensions are so small that the fabrication requires sophisticated technology. In the case of the image guide, the conductor loss is also a problem since the fields are quite strong on the ground plane. In the strip dielectric guide, the main flow of the electromagnetic waves lies in the dielectric layer away from the ground plane. Hence the loss is reduced considerably [4].

In this paper another new waveguide structure called double-layered slot line, which is believed to be useful in millimeter-wave IC applications, will be described. This structure is actually a modification of the conventional slot line originally proposed by Cohn [5]. In the conventional structure, the slot is made in the conducting ground plane placed on a dielectric substrate. In the new structure, shown in Fig. 1, the conventional slot line is modified by introducing an additional dielectric layer (region 2) between the ground plane and the substrate (region 3). By choosing the dielectric constant of region 3 larger than that of region 2, one can divert the electromagnetic energy flow away from the ground plane. Hence in the new structure the conductor loss can be reduced, and, at the same time, the ground plane provides a heat sink and is convenient for dc biasing in solid-state device application.

It should be noted that in the new structure the characteristic impedance is larger as compared with the single-layered line with the identical gap width $2w$. This effect is the consequence of the insertion of an additional dielectric layer which diverts the electromagnetic energy away from the conductor.

In the following sections, the propagation characteristics of this novel waveguide will be analyzed using an efficient numerical technique. Theoretical results will be compared with experimentally measured data. Furthermore, by numerically taking the limit of $h = 0$, the solution to the conventional slot line can be recovered. The results for this special case were compared with those available in the literature.

II. Formulation of the Problem

In the analysis the conductor thickness is considered to be negligible, and all the dielectric materials as well as the conductor are assumed to be lossless. The guided modes in the double-layered slot line structure are of hybrid nature. Hence the field components in each region of Fig. 1 may be written in terms of the electric and magnetic scalar potentials $\phi_i(x,y)$ and $\psi_i(x,y)$. For instance, omitting the propagation factor $\exp(-j\beta z)$,

$$E_{zi}(x,y) = j\frac{k_i^2 - \beta^2}{\beta}\phi_i(x,y) \tag{1a}$$

$$H_{zi}(x,y) = j\frac{k_i^2 - \beta^2}{\beta}\psi_i(x,y) \tag{1b}$$

$$E_{xi} = \frac{\partial}{\partial x}\phi_i(x,y) + \frac{\omega\mu_0}{\beta}\frac{\partial}{\partial y}\psi_i(x,y) \tag{1c}$$

$$H_{xi} = \frac{-\omega\varepsilon_{ri}\varepsilon_0}{\beta}\frac{\partial}{\partial y}\phi_i(x,y) + \frac{\partial}{\partial x}\psi_i(x,y), \qquad i = 1,2,3,4 \tag{1d}$$

where β is the propagation constant, ε_0 and μ_0 are the permittivity and the permeability of free space, respectively, and k_i and ε_{ri} are the wave number and the relative dielectric constant in region i. The scalar potentials ϕ_i and ψ_i satisfy the following equations:

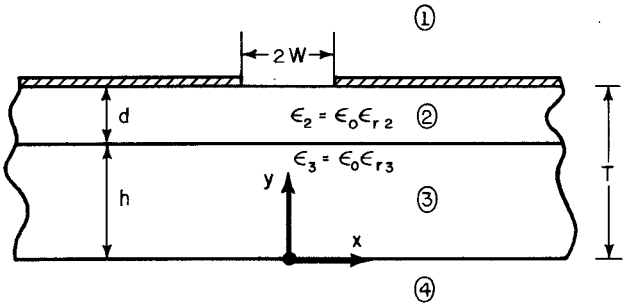

Fig. 1. Cross-sectional view of the double-layered slot line.

$$\nabla_t^2\phi_i(x,y) - (\beta^2 - k_i^2)\phi_i(x,y) = 0 \tag{2a}$$

$$\nabla_t^2\psi_i(x,y) - (\beta^2 - k_i^2)\psi_i(x,y) = 0 \tag{2b}$$

where ∇_t^2 implies the Laplacian with respect to the transverse (x and y) coordinates.

Although it is possible to solve these equations subject to the appropriate boundary conditions and to derive the eigenvalue equation for β, we will not proceed in this manner. Instead, we will use the Fourier transform or spectral domain technique, which has previously been applied to a number of problems on the slot line [6] and microstrip line structures [7], [8]. To this end, let us Fourier transform (2a) and (2b). We obtain

$$\frac{\partial^2\tilde{\phi}_i(\alpha,y)}{\partial y^2} - (\alpha^2 + \beta^2 - k_i^2)\tilde{\phi}_i(\alpha,y) = 0 \tag{3a}$$

$$\frac{\partial^2\tilde{\psi}_i(\alpha,y)}{\partial y^2} - (\alpha^2 + \beta^2 - k_i^2)\tilde{\psi}_i(\alpha,y) = 0 \tag{3b}$$

where $\tilde{\phi}_i$ and $\tilde{\psi}_i$ are the Fourier transforms of ϕ_i and ψ_i defined by

$$\tilde{\phi}_i(\alpha,y) = \int_{-\infty}^{+\infty}\phi_i(x,y)\exp(j\alpha x)\,dx \tag{4a}$$

$$\tilde{\psi}_i(\alpha,y) = \int_{-\infty}^{+\infty}\psi_i(x,y)\exp(j\alpha x)\,dx. \tag{4b}$$

The solutions of (3a) and (3b) are the superpositions of $\exp(\pm\gamma_i y)$ with unknown weight coefficients. Also,

$$\gamma_i = (\alpha^2 + \beta^2 - k_i^2)^{1/2}, \qquad i = 1,2,3,4$$

$$k_1 = k_4 = k_0 \qquad k_2 = \sqrt{\varepsilon_{r2}}\,k_0 \qquad k_3 = \sqrt{\varepsilon_{r3}}\,k_0$$

k_0 = free-space wave number.

We will now make use of the boundary and continuity conditions to derive the eigenvalue equation for the propagation constant β. Since the continuity conditions at $y = 0$ and $y = h$ are defined for all x in the space domain, they become after Fourier transformation

$$\begin{cases}\tilde{E}_{z4}(\alpha,0) = \tilde{E}_{z3}(\alpha,0) & \tilde{E}_{x4}(\alpha,0) = \tilde{E}_{x3}(\alpha,0)\\ \tilde{H}_{z4}(\alpha,0) = \tilde{H}_{z3}(\alpha,0) & \tilde{H}_{x4}(\alpha,0) = \tilde{H}_{x3}(\alpha,0)\end{cases} \tag{5a}$$

$$\begin{cases}\tilde{E}_{z3}(\alpha,h) = \tilde{E}_{z2}(\alpha,h) & \tilde{E}_{x3}(\alpha,h) = \tilde{E}_{x2}(\alpha,h)\\ \tilde{H}_{z3}(\alpha,h) = \tilde{H}_{z2}(\alpha,h) & \tilde{H}_{x3}(\alpha,h) = \tilde{H}_{x2}(\alpha,h).\end{cases} \tag{5b}$$

The application of the boundary and continuity conditions at the interface $y = h + d$ is more involved. In the space domain these conditions are given by

$$\text{(I)} \quad E_{z1}(x, h+d) = E_{z2}(x, h+d) = E_z(x)$$
$$E_{x1}(x, h+d) = E_{x2}(x, h+d) = E_x(x)$$
$$\text{(II)} \quad J_x(x) = H_{z1}(x, h+d) - H_{z2}(x, h+d)$$
$$J_z(x) = H_{x1}(x, h+d) - H_{x2}(x, h+d)$$

where

$$E_z(x) = \begin{cases} 0, & |x| > w \\ f(x), & |x| < w \end{cases} \qquad E_x(x) = \begin{cases} 0, & |x| > w \\ g(x), & |x| < w \end{cases} \tag{6a}$$

$$J_x(x) = \begin{cases} u(x), & |x| > w \\ 0, & |x| < w \end{cases} \qquad J_z(x) = \begin{cases} v(x), & |x| > w \\ 0, & |x| < w. \end{cases} \tag{6b}$$

The functions $f(x)$, $g(x)$, $u(x)$, and $v(x)$ are as yet unknown. In the Fourier transform domain, conditions (I) and (II) become

$$\text{(I')} \quad \tilde{E}_{z1}(\alpha, h+d) = \tilde{E}_{z2}(\alpha, h+d) = \tilde{E}_z(\alpha)$$
$$\tilde{E}_{x1}(\alpha, h+d) = \tilde{E}_{x2}(\alpha, h+d) = \tilde{E}_x(\alpha) \tag{7a}$$
$$\text{(II')} \quad \tilde{J}_x(\alpha) = \tilde{H}_{z1}(\alpha, h+d) - \tilde{H}_{z2}(\alpha, h+d)$$
$$\tilde{J}_z(\alpha) = \tilde{H}_{x1}(\alpha, h+d) - \tilde{H}_{x2}(\alpha, h+d) \tag{7b}$$

where $\tilde{E}_z$, $\tilde{E}_x$, $\tilde{J}_x$, and $\tilde{J}_z$ are the Fourier transforms of E_z, E_x, J_x, and J_z. For instance,

$$\tilde{E}_z = \int_{-\infty}^{\infty} E_z(x) \exp(j\alpha x)\, dx = \int_{-w}^{w} f(x) \exp(j\alpha x)\, dx.$$

Applying (5) and (7), we obtain the relations between $\tilde{J}_x, \tilde{J}_z$ and $\tilde{E}_z, \tilde{E}_x$

$$\tilde{J}_x(\alpha) = \tilde{G}_{11}(\alpha,\beta)\tilde{E}_z(\alpha) + \tilde{G}_{12}(\alpha,\beta)\tilde{E}_x(\alpha) \tag{8a}$$
$$\tilde{J}_z(\alpha) = \tilde{G}_{21}(\alpha,\beta)\tilde{E}_z(\alpha) + \tilde{G}_{22}(\alpha,\beta)\tilde{E}_x(\alpha) \tag{8b}$$

where $\tilde{G}_{11}(\alpha,\beta)$, etc., are known closed-form functions of α and β. It should be noted that they are actually the Fourier transforms of the diadic Green's function components in the space domain. Equations (8a) and (8b) have four unknowns, $\tilde{J}_x$, $\tilde{J}_z$, $\tilde{E}_z$, and $\tilde{E}_x$. However, because of the special nature of these equations, two of the unknowns, $\tilde{J}_x$ and $\tilde{J}_z$, can be eliminated in the following solution process. We now solve these equations by applying Galerkin's procedure.

First, let us expand unknown $\tilde{E}_z$ and $\tilde{E}_x$ in terms of known basis functions

$$\tilde{E}_z(\alpha) = \sum_{n=1}^{M} c_n \tilde{\xi}_n(\alpha) \tag{9a}$$

$$\tilde{E}_x(\alpha) = \sum_{n=1}^{N} d_n \tilde{\eta}_n(\alpha) \tag{9b}$$

where c_n and d_n are unknown coefficients. The basis functions must be chosen to be the Fourier transforms of functions which are identically zero for $|x| > w$. The application of Galerkin's procedure to (8) leads us to two simultaneous equations:

$$\sum_{n=1}^{M} c_n \int_{-\infty}^{\infty} \tilde{G}_{11}(\alpha,\beta)\tilde{\eta}_m(\alpha)\tilde{\xi}_n(\alpha)\, d\alpha + \sum_{n=1}^{N} d_n \int_{-\infty}^{\infty} \tilde{G}_{12}(\alpha,\beta)\tilde{\eta}_m(\alpha)\tilde{\eta}_n(\alpha)\, d\alpha = 0, \quad m = 1,2,3,\cdots,N \tag{10a}$$

$$\sum_{n=1}^{M} c_n \int_{-\infty}^{\infty} \tilde{G}_{21}(\alpha,\beta)\tilde{\xi}_k(\alpha)\tilde{\xi}_n(\alpha)\, d\alpha + \sum_{n=1}^{N} d_n \int_{-\infty}^{\infty} \tilde{G}_{22}(\alpha,\beta)\tilde{\xi}_k(\alpha)\tilde{\eta}_n(\alpha)\, d = 0, \quad k = 1,2,3,\cdots,M. \tag{10b}$$

The fact that the right-hand sides of these equations are zero may be verified by Parseval's relation

$$\int_{-\infty}^{\infty} \tilde{\eta}_m(\alpha)\tilde{J}_x(\alpha)\, d\alpha = \frac{1}{2\pi}\int_{-\infty}^{\infty} \eta_m(x)J_x(x)\, dx = 0 \tag{11}$$

because $\eta_m(x)$, the inverse transform of $\tilde{\eta}_m(\alpha)$, and $J_x(x)$ are nonzero only in the complementary regions of x. The propagation constant β can be obtained by solving the eigenvalue equation derivable by equating the determinant of the coefficient matrix of (10) to zero.

In actual computations, we have chosen $M = N = 1$ and the following forms have been used as the basis functions:

$$\tilde{\xi}_1(\alpha) = \frac{\pi w}{2}\frac{2}{\alpha} J_2(w|\alpha|) \tag{12a}$$

$$\tilde{\eta}_1(\alpha) = \frac{\pi w}{2} J_0(w|\alpha|) \tag{12b}$$

where J_0 and J_2 are the Bessel functions of order zero and two, respectively. The basis functions given by (12) are the transforms of the following functions:

$$\xi_1(x) = \begin{cases} -j\dfrac{x}{w}(w^2 - x^2)^{1/2}, & |x| \le w \\ 0, & |x| \ge w \end{cases} \tag{13a}$$

$$\eta_1(x) = \begin{cases} w(w^2 - x^2)^{-1/2}, & |x| \le w \\ 0, & |x| \ge w. \end{cases} \tag{13b}$$

Note that, by the preceding choice of the functions, the edge condition on the electromagnetic field is satisfied in the vicinity of the edges of the slot.

Before concluding this section, let us summarize some of the highlights of the present analysis method. First, the derivation of the transformed Green's function components is quite straightforward whereas in the space domain the Green's function takes a complex form, and, in fact, can be expressed in terms of the inverse transforms of the spectral domain counterparts and, hence, are of either integral or series form. This fact gives a number of advantages in numerical computation to the spectral domain technique. The second feature is that in the spectral domain

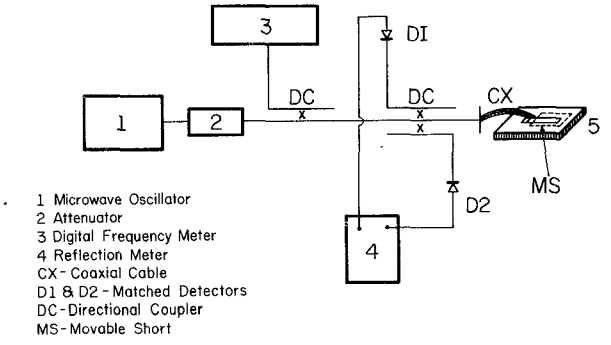

Fig. 2. Setup used for guide wavelength measurement.

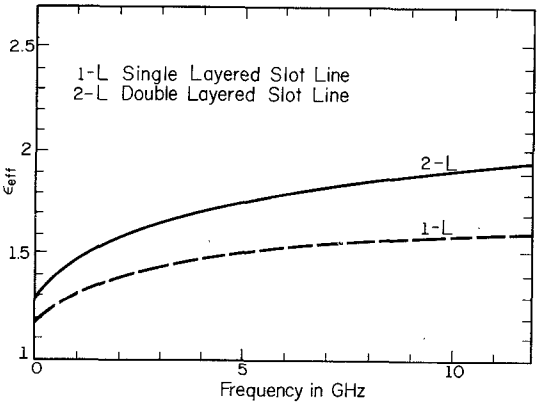

Fig. 3. Effective dielectric constant ε_{eff} versus frequency for the conventional (single-layered) and double-layered slot lines. $w = 1.0$ mm, $d = 3.2$ mm, $h = 5.0$ mm. $\varepsilon_{r2} = 2.55$ and $\varepsilon_{r3} = 2.62$ for the double-layered line. The single-layered line has the same dimensions except that $h = 0$.

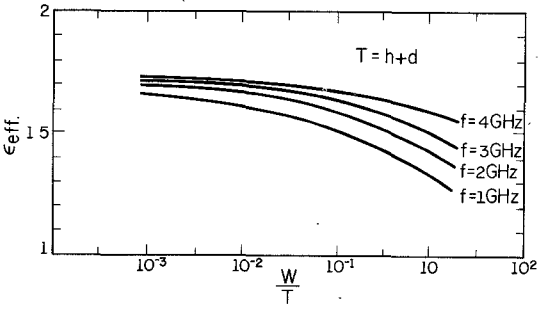

Fig. 4. Effective dielectric constant ε_{eff} of the double-layered slot line versus width at different frequencies. $d = 3.2$ mm, $h = 5.0$ mm, $\varepsilon_{r2} = 2.55$, and $\varepsilon_{r3} = 2.62$ for the double-layered lines. The single-layered line has the same dimension except $h = 0$.

formulation, the coupled pair of algebraic equations given by (8) is solved as opposed to the coupled integral equations of convolution type encountered in conventional space domain techniques. Again, this feature allows us to simplify the numerical processing. The matrix elements of (10) can be efficiently computed with the appropriate choice of basis functions such as those given by (12). Third, it is possible to systematically improve the numerical results by increasing the number of basis functions and by solving a larger size matrix equation.

III. Experiments

To check the theoretical results, a double-layered slot line was designed and fabricated to use at X band. The X band was chosen for experiments because of the better availability of the materials and the measuring equipment and of the ease of measurements. Region 2 is made of a polystyrene ($\varepsilon_{r2} = 2.55$) sheet of thickness $d = 3.2$ mm, and region 3 of a rexolite ($\varepsilon_{r3} = 2.62$) plate of thickness $h = 5.0$ mm. The upper surface of region 2 is coated with a thin copper foil in which a slot with width of $2w = 2$ mm is created.

The guide wavelength λ_g was measured using a setup described in Fig. 2. The slot line was excited either via a coaxial line or via an open-ended waveguide.

A movable short, which is a good conducting plate, is placed over the slot. When the position of the short across the slot is moved, the reflection coefficient of the slot line, seen from the external microwave source, changes, and the minimum occurs at each resonance length $l_n = n(\lambda_g/2)$, $n = 1,2,\cdots$. The positions of the short are recorded at two successive reflection minima. The distance between these positions gives the guide wavelength λ_g because

$$l_{n+1} - l_n = \lambda_g/2. \tag{14}$$

In the actual experiment we have measured more than two l_n and have used as experimental data the average of several λ_g values derived from (14).

IV. Results

The accuracy of the numerical process was confirmed first by solving the single-layered line for which h was numerically set to zero in the computer program and then by comparing the results with those available in the literature [5], [6]. It was found that the results obtained in this paper are indistinguishable from the curve given in [5] and [6].

Next, the effective dielectric constants defined via $\varepsilon_{eff} = (\beta/k)^2$ were computed and plotted in Fig. 3 for both the double-layered and the single-layered slot lines. Fig. 3 shows that ε_{eff} is higher for the double-layered structure, which means that the fields in the double-layered slot line are more concentrated in the dielectric region than in the conventional slot line. In fact, the major portion of the energy propagates in region 3 of the double-layered structure.

The variations of the effective dielectric constant ε_{eff} versus the slot width are presented in Fig. 4 for the double-layered slot line at a number of frequencies. Fig. 5 shows the guide wavelength λ_g in the double-layered line normalized by the free-space wavelength versus frequency. The theoretical and experimental results differ by less than 1 percent.

V. Conclusion

The double-layered slot line, which is believed to be useful for application in millimeter-wave IC's, is studied using Galerkin's method in the spectral domain. This method has a number of advantages over many conventional

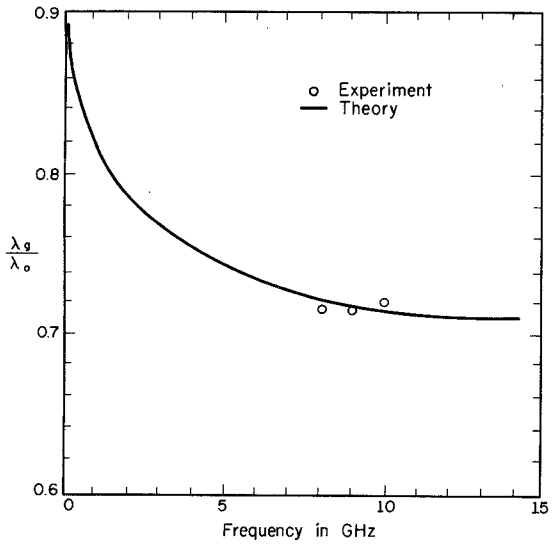

Fig. 5. Theoretical and experimental results of normalized guide wavelength of the double-layered slot line versus frequency. $w = 1.0$ mm, $d = 3.2$ mm, $h = 5.0$ mm, $\varepsilon_{r2} = 2.55$, and $\varepsilon_{r3} = 2.62$.

numerical techniques. The numerically obtained propagation constants for the dominant mode are found to be in good agreement with those obtained experimentally at X band. The computation time for evaluating a propagation constant for a given frequency is approximately 3.5 min on the G-20 computer, which is about 10 times slower than the IBM-360/75. Before this new waveguide is employed in the design of millimeter-wave IC's, extensive studies on the loss characteristics are needed.

References

[1] M. V. Schneider, "Millimeter-wave integrated circuits," 1973 IEEE International Microwave Symposium, Boulder, CO, June 4–6, 1973.
[2] P. P. Toulies and R. M. Knox, "Rectangular dielectric image lines for millimeter integrated circuits," 1970 Western Electric Show and Convention, Los Angeles, CA, August 25–28, 1970.
[3] H. Jacobs and M. M. Chrepta, "Electronic phase shifter for millimeter-wave semiconductor dielectric integrated circuits," *IEEE Trans. Microwave Theory Tech.*, vol. MTT-22, no. 4, pp. 411–417, April 1974.
[4] W. McLevige, T. Itoh, and R. Mittra, "New waveguide structures for millimeter-wave and optical integrated circuits," *IEEE Trans. Microwave Theory Tech.*, vol. MTT-23, no. 10, Oct. 1975.
[5] S. B. Cohn, "Slot line on a dielectric substrate," *IEEE Trans. Microwave Theory Tech.*, vol. MTT-17, no. 10, pp. 768–778, Oct. 1969.
[6] T. Itoh and R. Mittra, "Dispersion characteristics of slot lines," *Electron. Lett.*, vol. 7, no. 13, May 1973.
[7] T. Itoh and R. Mittra, "Spectral domain approach for calculating the dispersion characteristics of microstrip lines," *IEEE Trans. Microwave Theory Tech.*, vol. MTT-21, no. 7, pp. 496–499, July 1973
[8] T. Itoh, "Analysis of microstrip resonators," *IEEE Trans. Microwave Theory Tech.*, vol. MTT-22, no. 11, pp. 946–952, Nov. 1974.

80-GHz-Band Low-Loss Ring-Type Channel Diplexer Using a Semicircular Electric Mode

NOBUO NAKAJIMA AND ISAO OHTOMO, MEMBER, IEEE

***Abstract*—A low-loss ring-type channel diplexer consisting of two deformed ring cavities, three directional couplers, a TE_{01} mode semicircular waveguide for the through channels, and a TE_{10} mode rectangular waveguide for the dropped channel, has been developed as a channel-dropping filter for a millimeter-wave channel multiplexing network. The structure and experimental results of the diplexer are described, the design method is also discussed. Measurements show that insertion losses of the through and dropped (coupled) channels, and VSWR are less than 0.15 dB, 0.68 dB, and 1.12, respectively, for a diplexer centered at 81.91 GHz with 3-dB bandwidth of 800 MHz. Specifically, the through channel loss is reduced by half, as compared with a conventional rectangular waveguide diplexer, owing to the low insertion loss characteristics of the TE_{01} mode semicircular waveguide. As a result, an overall loss of a channel multiplexer, in which several channel diplexers are connected in tandem, is remarkably decreased, particularly at higher frequencies covering 80–120 GHz.**

Manuscript received January 29, 1976; revised May 4, 1976.
The authors are with the Yokosuka Electrical Communication Laboratory, Nippon Telegraph and Telephone Public Corporation, Yokosuka-shi 238-03, Japan.

I. Introduction

IN THE guided millimeter-wave transmission system under development in Japan, frequency ranges of 43–87 GHz [1] or more [2] are chosen in order to maintain the low loss of a millimeter-wave channel multiplexing network as well as of a circular waveguide medium. To realize such a network, several factors impose limitations on the choice of the filter structure and network construction.

There are physical limitations to the filter design at millimeter-wave frequencies because of the extremely small size. The feasibility of the filter fabrication must be considered. In addition, severe limitations exist in keeping the insertion loss low as the frequency increases. This means that hardware realization of the millimeter-wave channel multiplexing network is extremely difficult. Thus even waveguide filters of conventional structure can no longer meet the loss requirements of the guided millimeter-